

Supplementary Information

Simulated terrestrial runoff shifts the metabolic balance of a coastal Mediterranean plankton community toward heterotrophy

Tanguy Soulié¹, Francesca Vidussi¹, Justine Courboulès¹, Marie Heydon¹, Sébastien Mas², Florian Voron², Carolina Cantoni³, Fabien Joux⁴, Behzad Mostajir¹

¹MARBEC (MARine Biodiversity, Exploitation and Conservation), Univ Montpellier, CNRS, Ifremer, IRD, Montpellier, France

²MEDIMEER (MEDiterranean Platform for Marine Ecosystems Experimental Research), OSU OREME, CNRS, Univ Montpellier, IRD, INRAE, Sète, France

³CNR-ISMAR (Istituto di Scienze Marine), Area Science Park, Basovizza, Ed. Q2, Trieste, Italy

⁴Sorbonne Université, CNRS, Laboratoire d'Océanographie Microbienne (LOMIC), Observatoire Océanologique de Banyuls, Banyuls/Mer, France

Correspondence to: Tanguy Soulié (tanguy.soulie@gmail.com), Behzad Mostajir (behzad.mostajir@umontpellier.fr)

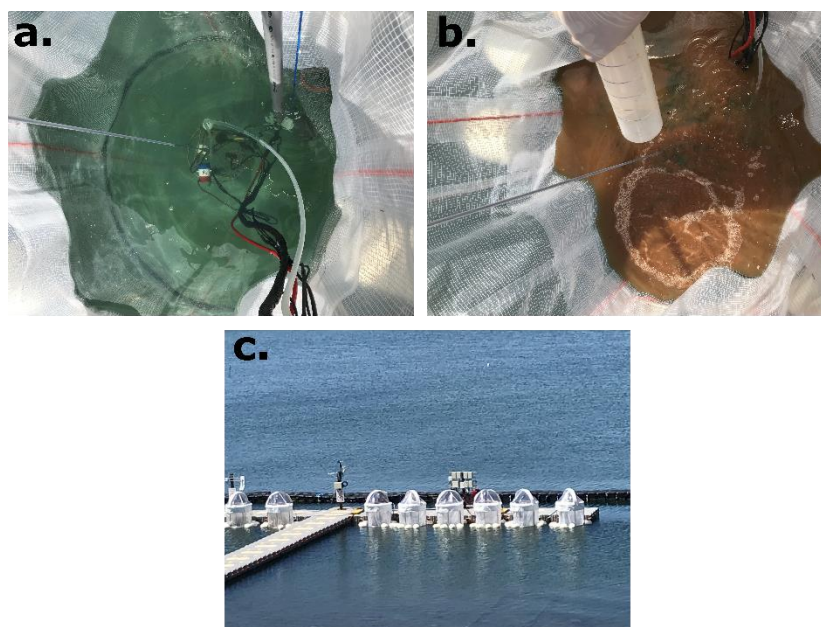


Figure S1. Pictures of (a.) the inside of a control mesocosm, (b.) the inside of a runoff mesocosm just after the addition of the maturated soil, and (c.) of the mesocosms and the surrounding lagoon. © Behzad Mostajir.

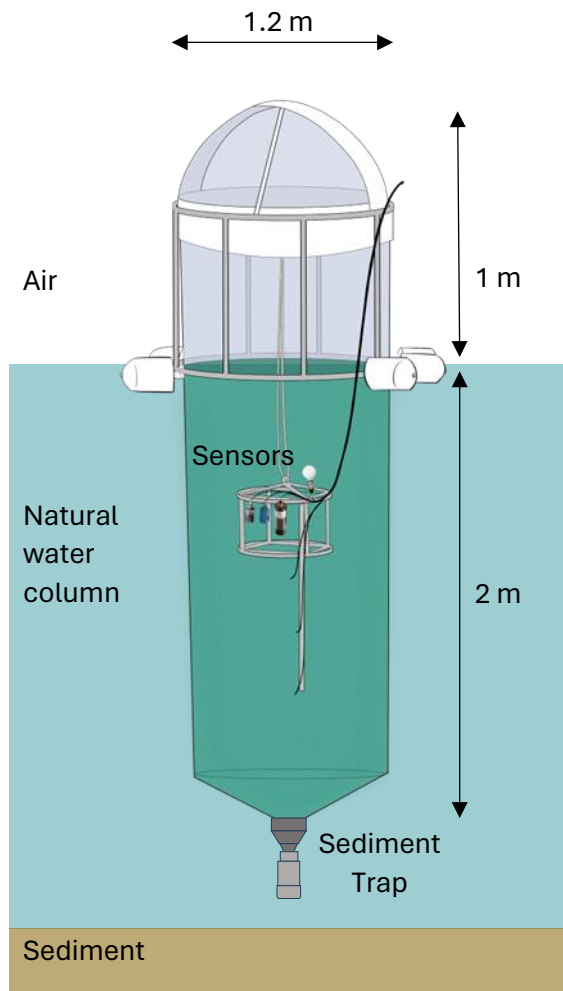


Figure S2. A schematic representation of a mesocosm unit and the set of automated sensors. © Justine Courboulès.

Calibration procedure of the high-frequency sensors

The fluorometers were calibrated with diluted and undiluted lagoon water with Chl-*a* concentrations, measured with a spectrofluorometer (LS 45, PerkinElmer, United States), ranging from 0 to 1.24 $\mu\text{g L}^{-1}$. In addition, the sensor Chl-*a* fluorescence was corrected with Chl-*a* concentrations measured daily and in each mesocosm using High Performance Liquid Chromatography (HPLC, Shimadzu, Nakagyo-ku, Japan) and the method of Zapata *et al.* (2000). Finally, the sensor Chl-*a* fluorescence data were corrected for non-photochemical quenching with a linear interpolation between sunrise and sunset (Soulié *et al.* 2022). These calibrated and corrected sensor Chl-*a* data are hereafter referred to as “Chl-*a*”. The oxygen optodes were calibrated at 0% and 100% saturation levels. The 0% saturation point was obtained by adding potassium metabisulfite into distilled water, and the 100% saturation point was reached by gently bubbling air into the distilled water. The sensor DO data were also corrected for temperature and salinity following the procedure detailed in Bittig *et al.* (2018). The sensor DO data were also corrected with DO concentrations measured daily and in each mesocosm using the Winkler method (Soulié *et al.* 2021). The conductivity sensors were calibrated with freshwater (salinity 0) and lagoon water (salinity 37.36). Finally, the water temperature probes were calibrated in a temperature-controlled water bath at 4 temperature levels, ranging from 10 to 25°C.

Estimation of phytoplankton growth and loss rates from high-frequency chlorophyll-*a* data

The high-frequency Chl-*a* data were used to estimate μ and L following a method detailed in Soulié *et al.* (2022). Each Chl-*a* cycle was separated in an “increasing period” and a “decreasing period”. The “increasing period” starts at sunrise until when the maximum Chl-*a* fluorescence is reached, generally a few minutes to a few hours after sunset. The “decreasing period” starts from this maximum until the next sunrise. For each period, an exponential fit was applied to the Chl-*a* data (**Eq. S1**):

$$Chla = a \times e^{bt}, \text{ (Equation S1)}$$

Where $Chla$ is the Chl-*a* in $\mu\text{g L}^{-1}$, a is a constant in $\mu\text{g L}^{-1}$ and b a constant in min^{-1} . Making the assumptions that Chl-*a* changes are only due to phytoplankton losses during the night and to both phytoplankton growth and losses during the day (Neveux *et al.* 2003), L and μ were estimated with **Eqs S2** and **S3**:

$$L = b_{dec}, \text{ (Equation S2)}$$

$$\mu = b_{inc} + L, \text{ (Equation S3)}$$

Where L and μ are phytoplankton loss and growth rates, respectively, in min^{-1} , and b_{dec} and b_{inc} the exponential coefficients of the fit during the “decreasing” and “increasing” periods, respectively. L was then converted to d^{-1} by multiplying it by 60 and 24, and μ was converted to d^{-1} by multiplying it by 60 and by the duration of the “increasing period” in h, as μ only occurs during this period.

Estimation of GPP and R from the high-frequency oxygen data

GPP and R were estimated from high-frequency dissolved oxygen data using a free-water diel oxygen method based on the classical technique from Odum (Odum 1956). Each dissolved oxygen cycle was separated in periods of positive instantaneous Net Community Production (NCP) and periods of negative instantaneous NCP (periods of increasing and decreasing dissolved oxygen concentration, respectively). For each positive and negative NCP periods, the dissolved oxygen data were smoothed with a 5-point sigmoidal model. The fundamental equation of the method is presented as **Eq. (S4)**:

$$\frac{\Delta O_2}{\Delta t} = GPP - R - F - A, \text{ (Equation S4)}$$

The instantaneous change in dissolved oxygen $\frac{\Delta O_2}{\Delta t}$ is considered to depend on GPP, R , and on F , which represents the physical oxygen exchange between the water and the atmosphere, and A , which encompasses all other phenomena which could affect the dissolved oxygen concentration. A was taken as null in the present work as in most other studies (Soulié *et al.* 2021). F was calculated as follows (**Eq. S5**):

$$F = (k \times (O_2 - O_{2sat}))/Z_{mix}, \text{ (Equation S5)}$$

In this equation, k represents the piston velocity coefficient, O_2 and O_{2sat} the concentration and saturation of dissolved oxygen respectively, and Z_{mix} the water column mixing depth,

which is the mesocosm water column length in the case of mixed mesocosms. The k value was taken as $k=0.000156 \text{ m min}^{-1}$ from the literature (Alcaraz *et al.* 2001). Then, k was corrected for temperature and salinity using the high-frequency sensors data and following the procedure described in Soulié *et al.* (2021). Then, instantaneous NCP was calculated from the following equation (Eq. S6):

$$NCP(t) = O_2(t) - O_2(t - 1) - F(t), \text{ (Equation S6)}$$

In this equation, $O_2(t)$ and $O_2(t - 1)$ are the dissolved oxygen concentration at time t and $t - 1$, respectively, and $F(t)$ the exchange factor at time t . From this instantaneous NCP data, daily metabolic parameters were inferred. First, the respiration occurring during daylight, R_{daytime} , was estimated with Eq. (S7):

$$R_{\text{daytime}} = (\text{mean of NCP during a 1h period centered around the max. NCP of the Negative NCP period}) \times \text{duration of Positive NCP period} \times 60, \text{ (Equation S7)}$$

In this equation, R_{daytime} is expressed in $\text{gO}_2 \text{ m}^{-3} \text{ d}^{-1}$, the mean instantaneous NCP in $\text{gO}_2 \text{ m}^{-3} \text{ min}^{-1}$, and the duration of the positive NCP period in h. The respiration occurring at night, R_{night} , was estimated from Eq. (S8):

$$R_{\text{night}} = (\text{mean of NCP during the Negative NCP period}) \times \text{duration of Negative NCP period} \times 60, \text{ (Equation S8)}$$

Similarly, R_{night} is expressed in $\text{gO}_2 \text{ m}^{-3} \text{ d}^{-1}$, the mean instantaneous NCP in $\text{gO}_2 \text{ m}^{-3} \text{ min}^{-1}$, and the duration of the negative NCP period in h. Finally, daily R is the sum of R_{daytime} and R_{night} . Daily GPP is then calculated with the following equation Eq. (S9):

$$GPP = R_{\text{daytime}} + (\text{mean of NCP during the Positive NCP period}) \times \text{duration of Positive NCP period} \times 60, \text{ (Equation S9)}$$

Daily GPP and R_{night} are expressed in $\text{gO}_2 \text{ m}^{-3} \text{ d}^{-1}$, the mean instantaneous NCP in $\text{gO}_2 \text{ m}^{-3} \text{ min}^{-1}$, and the duration of the positive NCP period in h. Daily NCP is then calculated as the difference between daily GPP and daily R .

References

- Alcaraz, M., Marrasé, C., Peters, F., Arin, L., and Malits, A.: Seawater-atmosphere O_2 exchange rates in open-top laboratory microcosms: application for continuous estimates of planktonic primary production and respiration. *J. Exp. Mar. Biol. Ecol.* **257**: 1-12. [https://doi.org/10.1016/S0022-0981\(00\)00328-2](https://doi.org/10.1016/S0022-0981(00)00328-2), 2001
- Bittig, H. C., Körtzinger, A., Neill, C., Van Ooijen, E., Plant, J. N., Hahn, J., Johnson, K. S., Yang, B., and Emerson, S. R.: Oxygen optode sensors: principle, characterization, calibration, and application in the Ocean. *Front. Mar. Sci.* **4**:429. <https://doi.org/10.3389/fmars.2017.00429>, 2018
- Neveux, J., Dupouy, C., Blanchot, J., Le Bouteiller, A., Landry, M. R., and Brown, S. L.: Diel dynamics of chlorophylls in high-nutrient, low-chlorophyll waters of the equatorial Pacific (180°): interactions of growth, grazing, physiological responses, and mixing. *J. Geophys. Res.* **108**:8240, <https://doi.org/10.1029/2000JC000747>, 2003
- Odum, H. T.: Primary production in flowing waters. *Limnol. Oceanogr.* **1**: 102-117. <https://doi.org/10.4319/lo.1956.1.2.0102>, 1956

- Soulié, T., Mas, S., Parin, D., Vidussi, F., and Mostajir, B.: A new method to estimate planktonic oxygen metabolism using high-frequency sensor measurements in mesocosm experiments and considering daytime and nighttime respirations. *Limnol. Oceanogr. Methods* **19**:303-316. <https://doi.org/10.1002/lom3.10424>, 2021
- Soulié, T., Vidussi, F., Mas, S., and Mostajir, B.: Functional stability of a coastal Mediterranean plankton community during an experimental marine heatwave. *Front. Mar. Sci.* **9**:831496. <https://doi.org/10.3389/fmars.2022.831496>, 2022
- Zapata, M., Rodriguez, F., and Garrido, J. L.: Separation of chlorophylls and carotenoids from marine phytoplankton: a new HPLC method using a reversed phase C8 column and pyridine-containing mobile phases. *Mar. Ecol. Prog. Ser.* **195**:29-45. <https://doi.org/10.3354/meps195029>, 2000